

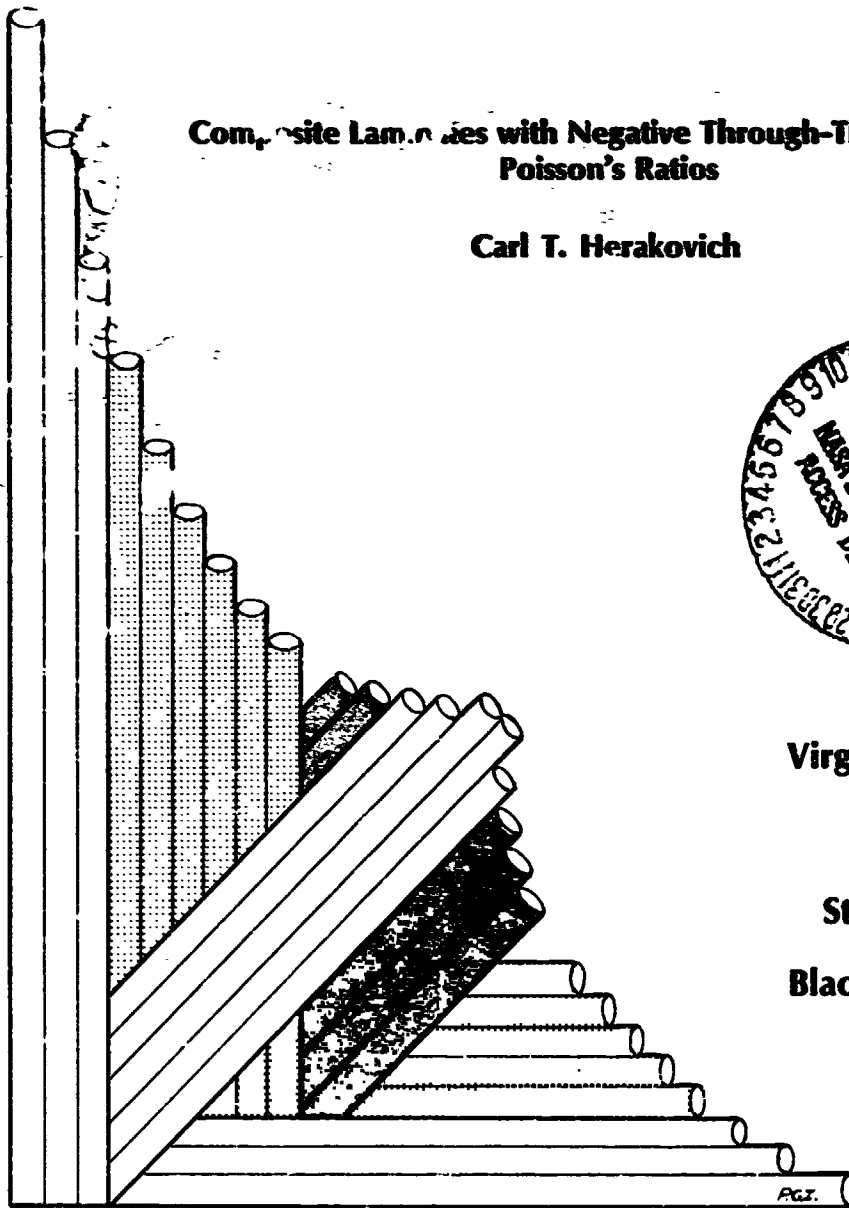
DRH

CCMS-84-01  
VPI-E-84-10

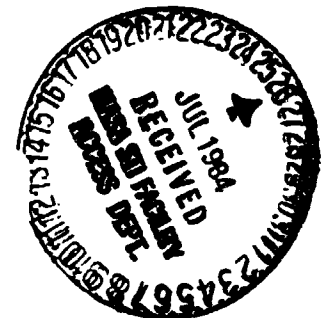
VIRGINIA TECH  
**CENTER FOR  
COMPOSITE MATERIALS  
AND STRUCTURES**

**Composite Laminates with Negative Through-The-Thickness  
Poisson's Ratios**

**Carl T. Herakovich**



**Virginia Polytechnic  
Institute  
and  
State University  
Blacksburg, Virginia  
24061**



(NASA-CR-173681) COMPOSITE LAMINATES WITH  
NEGATIVE THROUGH-THE-THICKNESS POISSON'S  
RATIOS (Virginia Polytechnic Inst. and State  
Univ.) 20 p HC A02/MF A01 CACL 11D

N84-27830

Unclas  
G3/24 00868

College of Engineering  
Virginia Polytechnic Institute and State University  
Blacksburg, VA 24061

VPI-E-84-10

April, 1984

Composite Laminates with Negative  
Through-the-Thickness  
Poisson's Ratios

Carl T. Herakovich\*

Department of Engineering Science & Mechanics

Interim Report 39  
The NASA-Virginia Tech Composites Program

NASA Cooperative Agreement NAG-1-343.

Prepared for: Applied Materials Branch  
National Aeronautics & Space Administration  
Langley Research Center  
Hampton, VA 23665

\*Professor of Engineering Science & Mechanics

## INTRODUCTION

The through-the-thickness effective poisson's ratio of a composite laminate can be an important property in the application and testing of composite materials. Thickness changes can influence the gripping force on test specimens and the measurement of transverse displacements. They have the potential to have a critical effect on structures requiring a high degree of dimensional stability such as optical benches, space telescopes and antennas, and joints. Further, thickness changes can be very important to the performance of bonded and bolted joints. However, little if any attention has been given to this laminate property. In fact, no references to the subject were found in the literature during the preparation of this manuscript.

Negative in-plane poisson's ratios  $\nu_{xy}$  have been reported previously [1] and negative average through-the-thickness poisson's ratios on the free edge of laminates have been measured [2]. These negative values of the free edge were shown to correlate well with finite element results. However, no attempt was made to study the general laminate behavior away from edges. As will be shown, there is a significant difference between the behavior in interior regions and that at the free edge. Negative poisson's ratios have also been reported for a small number of other materials [3].

It should be emphasized that the effective poisson's ratio is a laminate (or structural) property and not a material property. As will be demonstrated, it is a function of the internal stress state in the

laminate. Henceforth in this paper, the term poisson's ratio will be used to imply the effective laminate property.

### PROBLEM FORMULATION

The magnitude of the through-the-thickness poisson's ratio  $\nu_{xz}$  can be predicted quite easily through a combination of lamination theory and the appropriate three-dimensional constitutive equation. Consider a symmetric composite laminate under axial load  $N_x$  (Fig. 1). Lamination theory gives the midplane strains

$$\begin{pmatrix} \epsilon_x \\ \epsilon_y \\ \gamma_{xy} \end{pmatrix} = \begin{bmatrix} A_{11} & A_{12} & A_{16} \\ A_{12} & A_{22} & A_{26} \\ A_{16} & A_{26} & A_{66} \end{bmatrix}^{-1} \begin{pmatrix} N_x \\ 0 \\ 0 \end{pmatrix} \quad (1)$$

where  $A_{ij} = \sum_{k=1}^N \bar{Q}_{ij}^k t^k$ ,  $\bar{Q}_{ij}^k$  are coefficients of the reduced stiffness matrix,  $t^k$  are the individual layer thicknesses and  $N$  is the number of plies. The through-the-thickness poisson's ratio is defined

$$\nu_{xz} = \frac{-\epsilon_z}{\epsilon_x} \quad (2)$$

where the strain  $\epsilon_z$  equals the total transverse displacement  $W$  divided by the laminate thickness  $2H$ . The total  $W$  displacement can be written

$$W = \int_{-H}^H \epsilon_z dz = \sum_{k=1}^N \epsilon_z^k t^k \quad (3)$$

where  $\epsilon_z^k$  is the constant strain in the  $k^{\text{th}}$  layer. The strain  $\epsilon_z^k$  in any layer can be determined using the three-dimensional constitutive equation for a monoclinic (off-axis) layer

$$\epsilon_z^k = \bar{S}_{31}^k \sigma_x^k + \bar{S}_{32}^k \sigma_y^k + \bar{S}_{33}^k \sigma_z^k + \bar{S}_{36}^k \tau_{xy}^k \quad (4)$$

where the  $\bar{S}_{ij}$  are the coefficients of the transformed 3-D compliance matrix.

Away from free edges, the laminate is in a state of plane stress and hence  $\sigma_z^k$  is zero. Thus,  $\epsilon_z^k$  in each layer is

$$\epsilon_z^k = \bar{S}_{31}^k \sigma_x^k + \bar{S}_{32}^k \sigma_y^k + \bar{S}_{36}^k \tau_{xy}^k \quad (5)$$

The stresses in each layer can be determined from two-dimensional constitutive equations and the inverse of  $A_{ij}$  as

$$\begin{pmatrix} \sigma_x \\ \sigma_y \\ \tau_{xy} \end{pmatrix}^k = \begin{bmatrix} \bar{Q}_{11} & \bar{Q}_{12} & \bar{Q}_{16} \\ \bar{Q}_{12} & \bar{Q}_{22} & \bar{Q}_{26} \\ \bar{Q}_{16} & \bar{Q}_{26} & \bar{Q}_{66} \end{bmatrix}^k \begin{pmatrix} A_{11}^{-1} \\ A_{12}^{-1} \\ A_{16}^{-1} \end{pmatrix} N_x \quad (6)$$

Substituting (6) into (5) gives  $\epsilon_z^k$  in each layer in terms of material and laminate properties and the applied load

$$\begin{aligned}
\epsilon_z^k = N_x [ & A_{11}^{-1} (\bar{S}_{31}^k \bar{Q}_{11}^k + \bar{S}_{32}^k \bar{Q}_{12}^k + \bar{S}_{36}^k \bar{Q}_{16}^k) \\
& + A_{12}^{-1} (\bar{S}_{31}^k \bar{Q}_{12}^k + \bar{S}_{32}^k \bar{Q}_{22}^k + \bar{S}_{36}^k \bar{Q}_{26}^k) \\
& + A_{16}^{-1} (\bar{S}_{31}^k \bar{Q}_{16}^k + \bar{S}_{32}^k \bar{Q}_{26}^k + \bar{S}_{36}^k \bar{Q}_{66}^k) ]
\end{aligned} \tag{7}$$

Combining (3) and (7) gives the total W displacement

$$\begin{aligned}
W = N_x [ & A_{11}^{-1} \sum_{k=1}^N (\bar{S}_{31}^k \bar{Q}_{11}^k + \bar{S}_{32}^k \bar{Q}_{12}^k + \bar{S}_{36}^k \bar{Q}_{16}^k) t^k \\
& + A_{12}^{-1} \sum_{k=1}^N (\bar{S}_{31}^k \bar{Q}_{12}^k + \bar{S}_{32}^k \bar{Q}_{22}^k + \bar{S}_{36}^k \bar{Q}_{26}^k) t^k \\
& + A_{16}^{-1} \sum_{k=1}^N (\bar{S}_{31}^k \bar{Q}_{16}^k + \bar{S}_{32}^k \bar{Q}_{26}^k + \bar{S}_{36}^k \bar{Q}_{66}^k) t^k ]
\end{aligned} \tag{8}$$

And dividing by the applied axial strain  $\epsilon_x$  (Eqn. 1) and the thickness  $2H$  provides the expression for the through-the-thickness poisson's ratio

$$\begin{aligned}
\nu_{xz} = \frac{-1}{2HA_{11}^{-1}} [ & A_{11}^{-1} \sum_{k=1}^N (\bar{S}_{31}^k \bar{Q}_{11}^k + \bar{S}_{32}^k \bar{Q}_{12}^k + \bar{S}_{36}^k \bar{Q}_{16}^k) t^k \\
& + A_{12}^{-1} \sum_{k=1}^N (\bar{S}_{31}^k \bar{Q}_{12}^k + \bar{S}_{32}^k \bar{Q}_{22}^k + \bar{S}_{36}^k \bar{Q}_{26}^k) t^k \\
& + A_{16}^{-1} \sum_{k=1}^N (\bar{S}_{31}^k \bar{Q}_{16}^k + \bar{S}_{32}^k \bar{Q}_{26}^k + \bar{S}_{36}^k \bar{Q}_{66}^k) t^k ]
\end{aligned} \tag{9}$$

Defining

$$F_i = \sum_{k=1}^N (S_{31} Q_{i1} + S_{32} Q_{i2} + S_{36} Q_{i6}) \quad (i = 1, 2, 6) \tag{10}$$

we can write

$$v_{xz} = \frac{-1}{2HA_{11}^{-1}} [A_{11}^{-1}F_1 + A_{12}^{-1}F_2 + A_{16}^{-1}F_6] \quad (11)$$

A similar development for axial loading  $N_y$  gives the through-the-thickness poisson's ratio  $v_{yz}$

$$v_{yz} = \frac{-1}{2HA_{22}^{-1}} [A_{21}^{-1}F_1 + A_{22}^{-1}F_2 + A_{26}^{-1}F_6] \quad (12)$$

Equations (11 and (12) can be written in condensed notation

$$v_{xz} = \frac{-1}{2HA_{11}^{-1}} [A_{1i}^{-1}F_i] \quad (13)$$

$$v_{yz} = \frac{-1}{2HA_{22}^{-1}} [A_{2i}^{-1}F_i] \quad (i = 1,2,6)$$

where summation of the repeated subscript  $i$  is implied.

## RESULTS

Typical results for T300/5208 graphite-epoxy are shown in Fig. 2. The figure shows a plot of the variation in  $v_{xz}$  for unidirectional off-axis laminae and angle-ply laminates ( $[\pm\theta]_s$ ) with fiber orientations ranging from 0 to 90 degrees. It can be seen that  $v_{xz}$  varies radically with fiber orientation in angle-ply laminates, attaining a minimum negative value of -0.21 for a  $[\pm 25]_s$  laminate compared to a maximum

positive value of 0.49 for a [90] laminate. The negative poisson's ratios for angle-ply laminates with fiber orientations between  $15^\circ$  and  $40^\circ$  is due to the high degree of normal-shear coupling (non-zero  $\bar{Q}_{16}^k$ ) and the constraining influence of adjacent layers. The coupling results in high inplane shear stresses and a lateral poisson's ratio  $\nu_{xy}$  greater than 1.0 [1]. A lateral poisson's ratio greater than one and a negative through-the-thickness poisson's ratio are physically consistent.

The through-the-thickness poisson's ratio for angle-ply laminates differs drastically from that for off-axis lamina (Fig. 2) much like the inplane poisson's ratio of the laminate differs from that of the lamina [1]. Both results show clearly that a laminated composite is a structure whose elastic constants cannot be determined by a simple rule of mixtures. In fact  $\nu_{xz}$  is an even function of  $\theta$  for unidirectional off-axis laminae and thus is positive for both plus and minus fiber orientations. And yet the combination of plus and minus theta layers has a negative poisson's ratio. This result is a clear indication that all interactions between constraining layers must be properly accounted for.

Results for  $\nu_{yz}$  of angle-ply laminates are shown in Fig. 3. They correspond to a reflection of the  $\nu_{xz}$  results about the  $45^\circ$  orientation.

The underlying physics of the negative poisson's ratio phenomenon may be better understood through consideration of the plane stress expression for the through-the thickness strain in material principal coordinates



$$\epsilon_3 \equiv e_z = \frac{-\nu_{13}\sigma_1}{E_1} - \frac{\nu_{23}\sigma_2}{E_2} \quad (14)$$

From Eq. (14) it is evident that  $\epsilon_z$  can be negative if either  $\sigma_1$  or  $\sigma_2$  is compressive and of sufficient magnitude. For angle-ply laminates,  $\sigma_1$  is a constant tensile value and  $\sigma_2$  is a constant compressive value for all layers (Fig. 4). In the fiber orientation range  $15^\circ$ - $40^\circ$ , the magnitude of  $\sigma_2$  is sufficiently large to render  $\epsilon_z$  positive for all layers of the laminate.

Figure 5 shows through-the-thickness poisson's ratios for  $[0/\pm\theta]_s$  and  $[0_2/\pm\theta]_s$  laminates compared to the results for the laminae and angle-ply laminates of Fig. 2. Clearly, negative through-the-thickness poisson's ratios are not limited to  $[\pm\theta]_s$  angle-ply laminates. There is a wide variety of  $[0_2/\pm\theta]_s$  and  $[0/\pm\theta]_s$  laminates which have negative poisson's ratios  $\nu_{xz}$ . These curves show the influence of fiber orientation as well as the influence of the percent  $0^\circ$  layers. They also show that there is a wide variety of laminates which can be tailored to have a zero through-the-thickness poisson's ratio.

The  $[0_2/\pm 90]_s$  laminate is equivalent to the cross-ply laminate  $[0_2/90_2]_s$ . Its  $\nu_{xz}$  is 0.413. Also shown for comparison is the through-the-thickness poisson's ratio for a quasi-isotropic  $[0/\pm 45/90]_s$  laminates ( $\nu_{xz} = 0.301$ ). It is interesting that the  $[0/\pm 45/90]_s$  quasi-isotropic laminate has the same through-the-thickness poisson's ratio as the  $[0/\pm 60]_s$  quasi-isotropic laminate. It should be noted that all laminate results are independent of stacking sequence for symmetric laminates.

As mentioned previously, the analysis presented is valid only away from free edges. The influence of edge effects is demonstrated in Fig. 6. Figure 6a shows the in-plane  $(v,w)$  displacements (not to scale) in a quarter section of a  $[30_2/-30_2]_S$  laminate under tensile axial load  $N_x$  as obtained using finite elements [4]. (All finite element plots have been normalized for a uniform maximum deformation). Both undeformed and deformed shapes are indicated in the figure. It is evident that the laminate is thicker under load in interior regions away from the edge corresponding to a negative poisson's ratio as predicted by the simplified analysis of Eqns. 1-13. It is also interesting to note that the opposite is true in the boundary layer along the free edge where the complex triaxial stress state results in a variable poisson's ratio which attains a maximum positive value at the free edge. It is important to note that the simplified analysis of Eqns. 1-13 and the elasticity solution of the finite element analysis give the same result in interior regions.

Unlike interior regions, the thickness changes in the boundary layer region are a function of the laminate stacking sequence. This is demonstrated more dramatically in Figs. 6b and 6c where the deformed shapes of two quasi-isotropic laminates of different stacking sequence are shown. Both laminates have identical thickness changes in interior regions, but entirely different deformed shapes in the boundary layer region. The  $[0/-45/0/45]_S$  laminate has a positive  $v_{xz}$  at the free edge, but the  $[+45/0/90]_S$  laminate has a small negative  $v_{xz}$  at the free edge. Obviously, the stacking sequence plays a dominant role in the

boundary layer region. These results are consistent with those presented in reference [2].

Another interesting feature of the results presented here is the influence of the fiber orientation in angle-ply laminates on the dilatation  $e = \epsilon_x + \epsilon_y + \epsilon_z$ . The laminate dilatation can be positive or negative depending on fiber orientation. For example, a  $[\pm 10]_S$  laminate has a positive dilatation  $e = 0.32\epsilon_x$  whereas a  $[\pm 30]_S$  laminate has a negative dilatation  $e = -0.32\epsilon_x$ . Thus it is possible to tailor the dilatation of a composite laminate over a range of values including zero. This compares to the positive dilatation of a typical metal ( $\nu = 0.3$ ) of  $e = 0.4\epsilon_x$ .

#### CONCLUDING REMARKS

It has been shown that the through-the-thickness poisson's ratios of graphite-epoxy angle-ply and related laminates exhibit a wide range of values including relatively large negative values for laminates having layers with high normal-shear coupling. Poisson's ratios which are negative in one plane, but greater than 1.0 in an orthogonal plane are unique to anisotropic, layered materials. It may be surprising to engineers and scientists unfamiliar with these materials that such properties are possible. Lateral poisson's ratios greater than one have been measured in the laboratory. To this authors knowledge, no attempt has been made to measure the through-the-thickness poisson's ratio away from edges.

Since the laminates studied here are symmetric and subjected to inplane loading, the results are independent of laminate stacking sequence (away from edges). Similarly unusual results are to be expected for other properties such as the through-the-thickness coefficients of thermal and hygroscopic expansion.

Finally, the ability to tailor materials to have negative or zero poisson's ratios and negative or zero dilatation presents some exciting possibilities for innovative uses of these materials.

#### ACKNOWLEDGEMENT

This work was supported by the NASA-Virginia Tech Composites Program, NASA Grant NAG-1-343. The author would like to express his appreciation to all Virginia Tech faculty and students who have shared their ideas and especially Professor Michael Hyer for helpful discussions during the course of this study.

#### REFERENCES

1. Tsai, S. W. and Hahn, H. T., Introduction to Composite Materials, Technomic, Westport, CT, 1980.
2. Bjeletich, J. G., Crossman, F. W. and Warren, W. J., "The Influence of Stacking Sequence on Failure Modes in Quasi-Isotropic Graphite-epoxy Laminates," Failure Modes in Composites IV, (Cornie and Crossman, eds.), The Metallurgical Society of AIME, 1977.
3. Simmons, G. and Wang, H., Single Crystal Elastic Constants and Calculated Aggregate Properties: A Handbook, M.I.T. Press, Cambridge, Mass. 1971.
4. Buczek, M. B., Gregory, M. A., Herakovich, C. T., "CLFE2D--A Generalized Plain Strain Finite Element Program for Laminated Composites Subjected to Mechanical and Hygrothermal Loading," VPI-E-83-40, Virginia Polytechnic Institute and State University, October 1983.

ORIGINAL PAGE IS  
OF POOR QUALITY

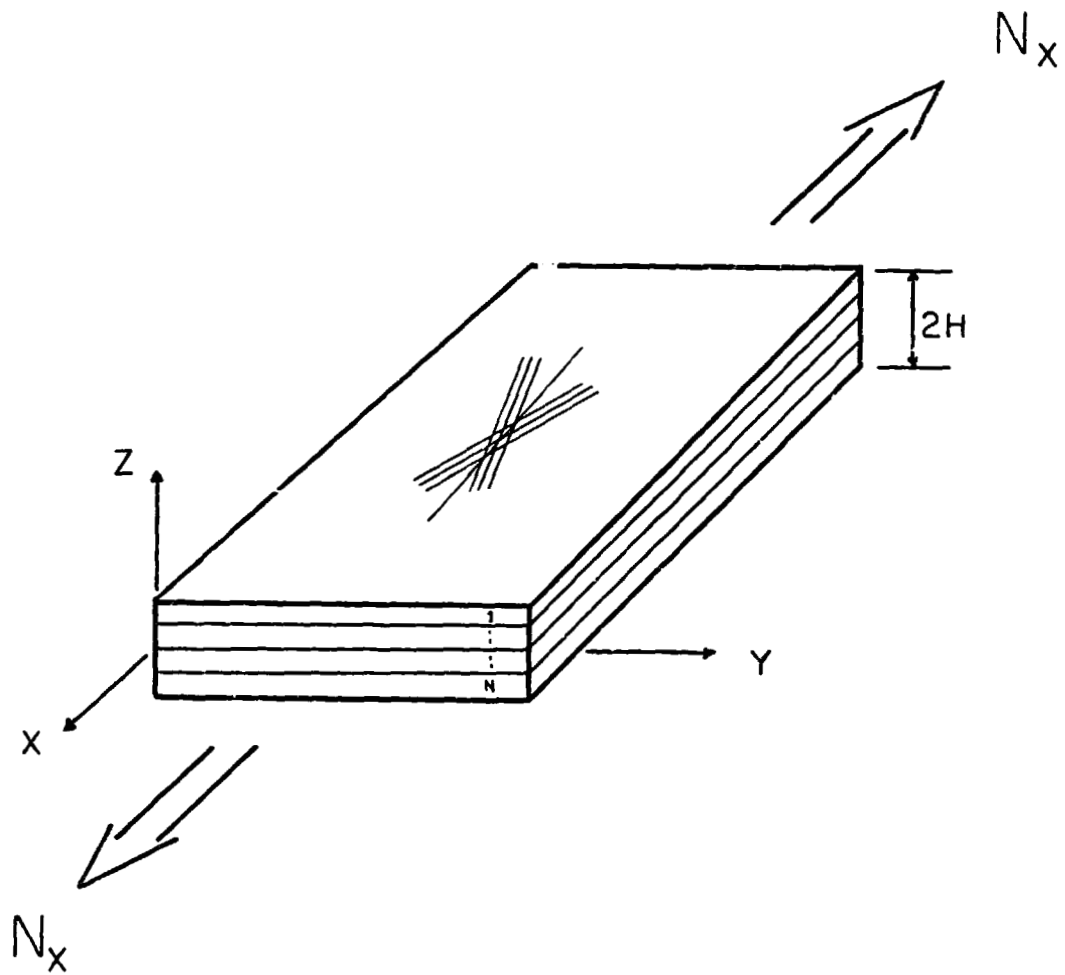


FIG.1. LAMINATE UNDER AXIAL LOAD

ORIGINAL PAGE IS  
OF POOR QUALITY

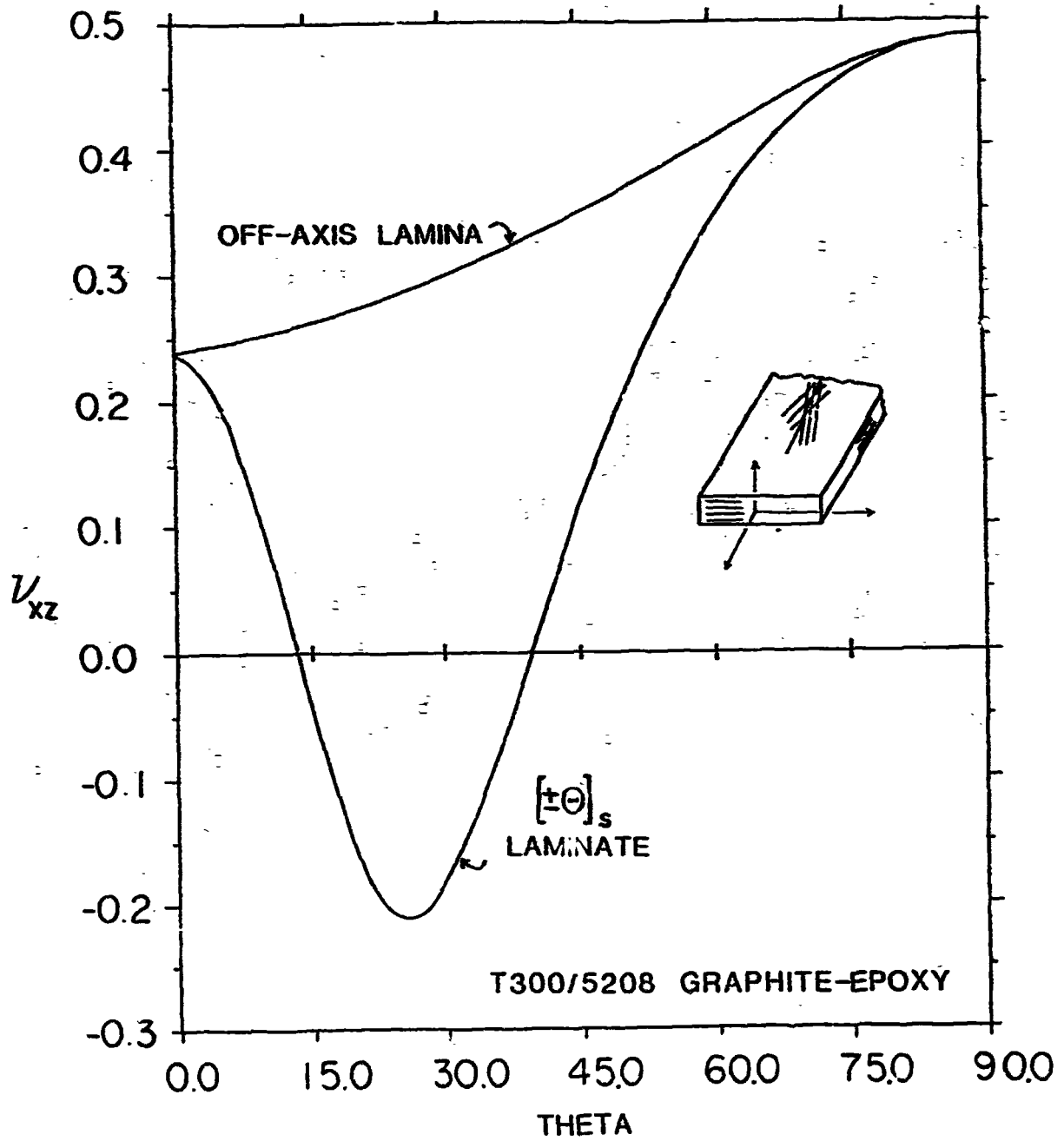


FIG.2.  $\nu_{xz}$  FOR ANGLE-PLY AND OFF-AXIS LAMINA

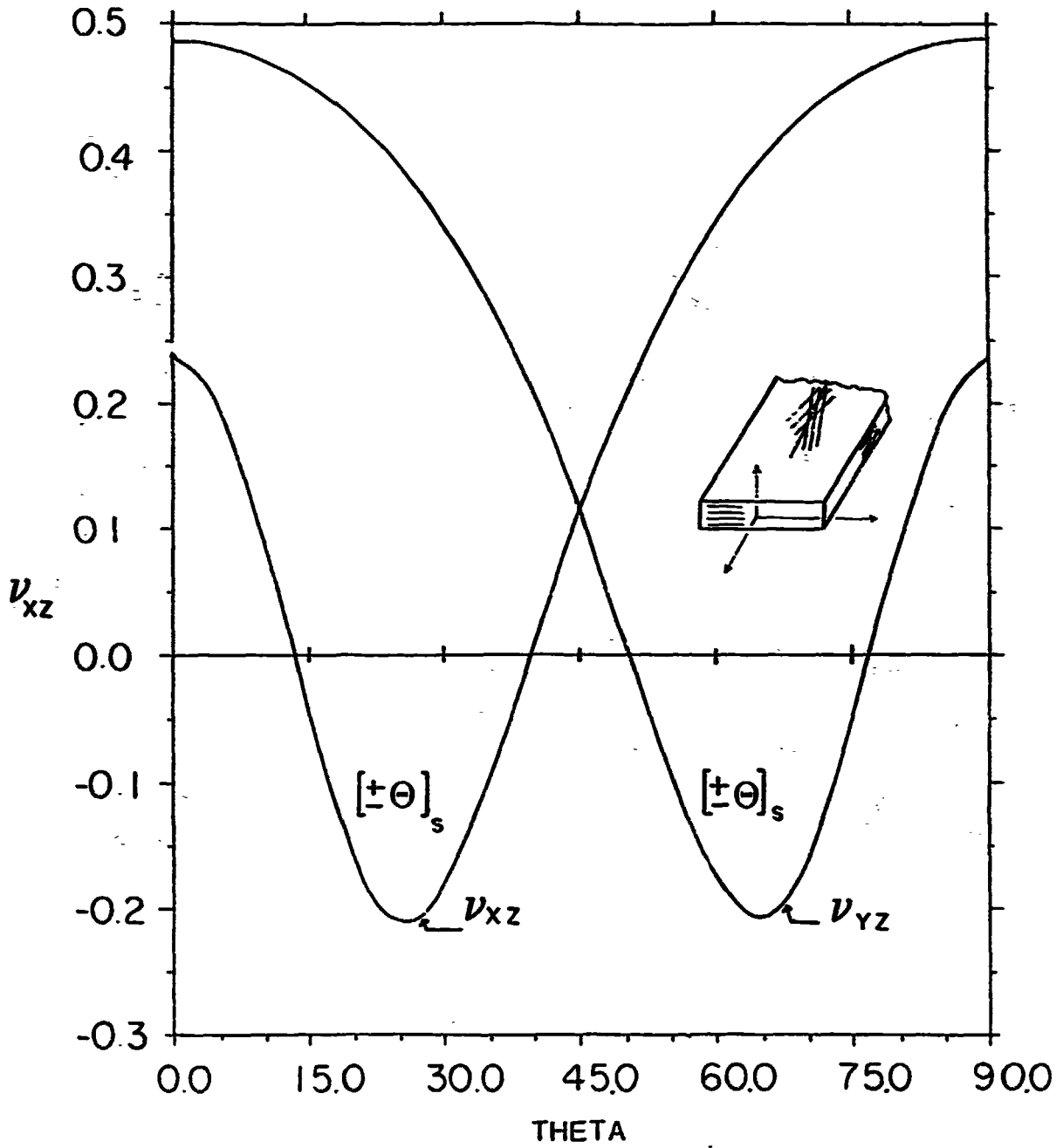


FIG.3.  $\nu_{xz}$  AND  $\nu_{yz}$  FOR ANGLE-PLY LAMINATES

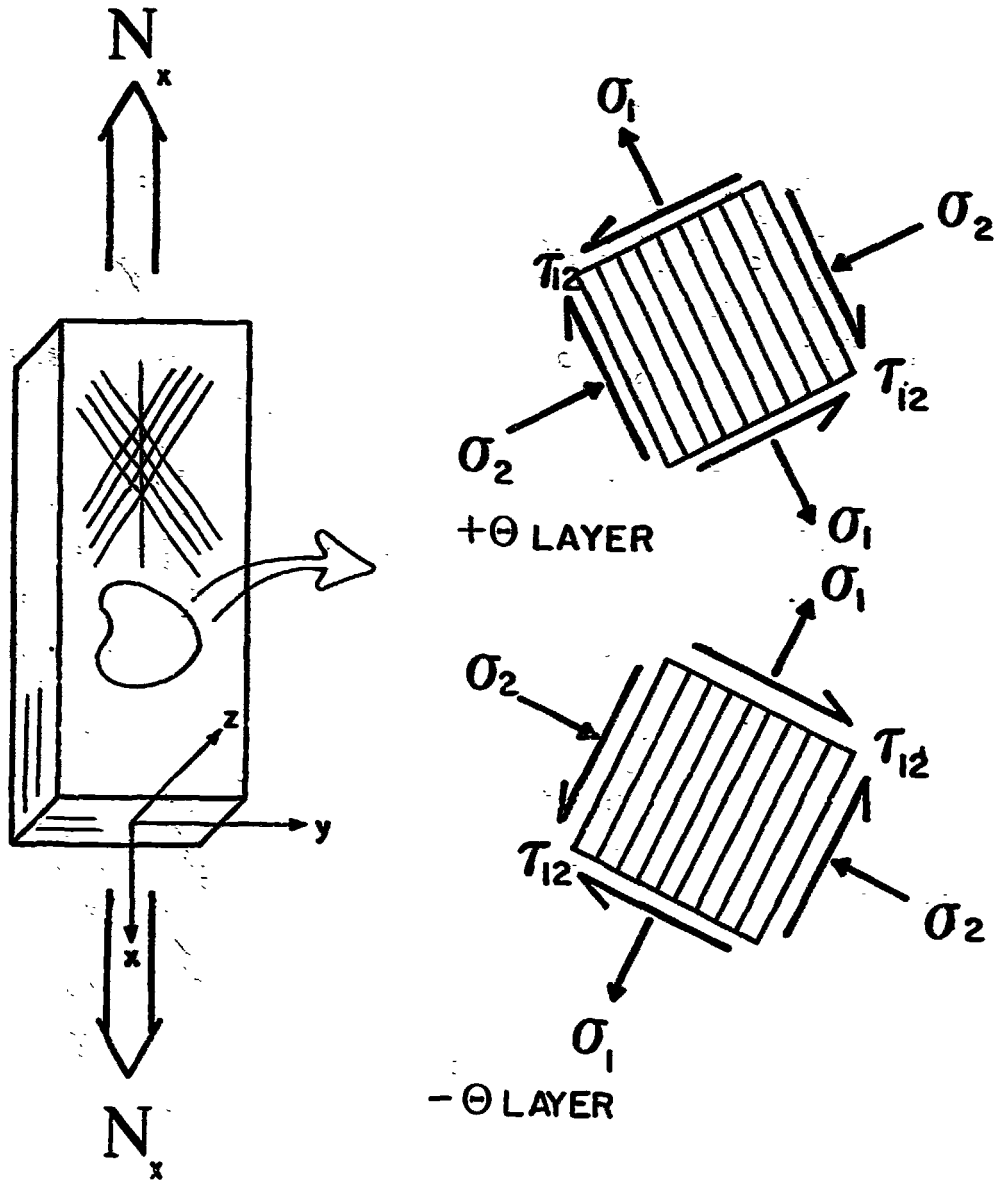


FIG.4. STRESS STATES IN ANGLE-PLY LAMINATES



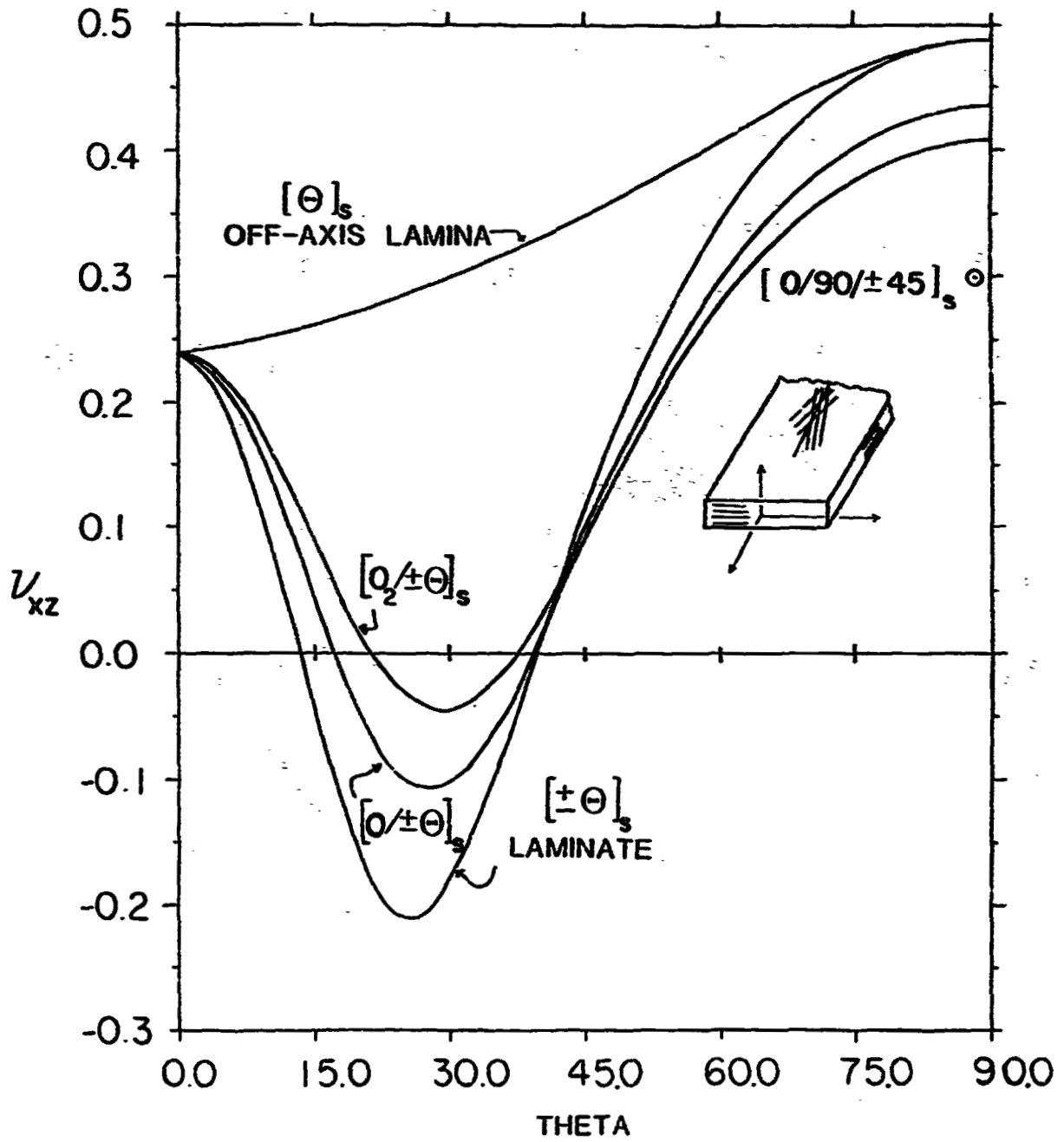


FIG.5.  $V_{xz}$  FOR  $[0_n / \pm \theta]_s$  AND OTHER LAMINATES

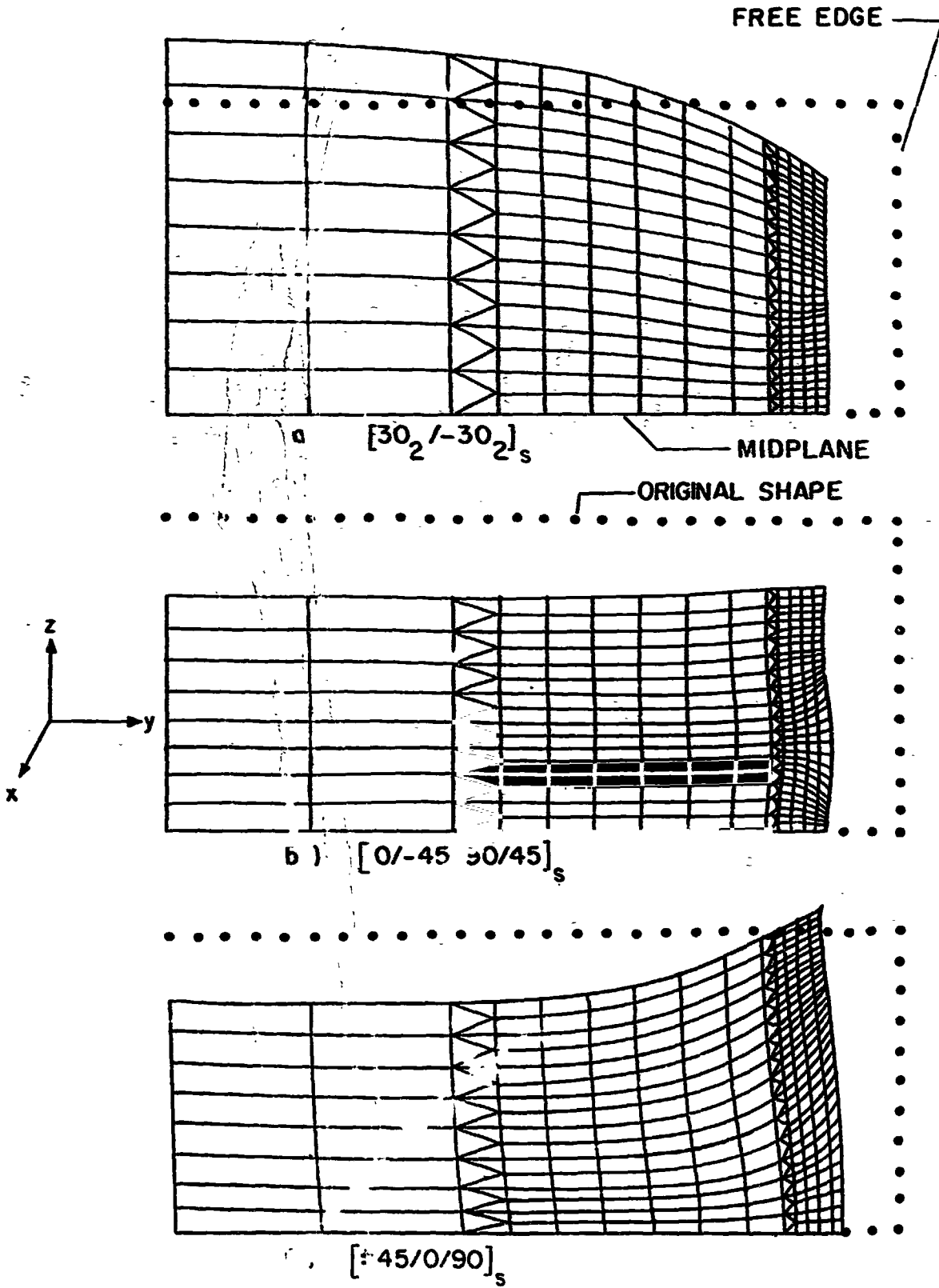


FIG.6. THICKNESS CHANGES IN BOUNDARY LAYER